Kathmandu University
Journal of Science, Engineering and Technology

Development and characterization of sustainable clay-cement composite bricks reinforced with coconut fibre and rice husk ash

Kabiru Mustapha* [a], Sikiru Ottan Abdulraman [b], Suraju Adesina Adepoju [c], and Oluwatosin Eunice Egbanubi [d]

[a]Department of Materials Science and Engineering, Kwara State University, Malete, Nigeria.
[b]Department of Mining Engineering, Kwara State University, Malete, Nigeria.
[c]Department of Geology and Minerals Sciences, Kwara State University, Malete, Nigeria.
[d]Department of Chemical Engineering, University of Ilorin, Nigeria.

Abstract

This study investigates the development of clay-cement composites reinforced with coconut fibre and cement partially replaced with rice husk ash (RHA) for brick applications. Conventional fired and unfired clay bricks are often limited by high energy consumption, environmental impact, and low mechanical strength. To address these challenges, this study explores the incorporation of agricultural wastes (coconut fibre) and RHA to enhanced mechanical and microstructural performance. Clay-based composite bricks were developed by partially replacing cement with rice husk ash (RHA) and reinforcing the mixture with 0–25 vol.% coconut fibre. The composite system incorporates coconut fibre as the primary reinforcement, while rice husk ash functions solely as a pozzolanic partial replacement for cement. Physical, chemical and microstructural characterization of the clay and RHA was conducted using hydrometer analysis, X-Ray Diffraction (XRD), X-Ray Fluorescence (XRF), and Scanning Electron Microscopy (SEM). The XRD analysis revealed that the clay was rich in kaolinite, while RHA contained 66.95% SiO_2, providing pozzolanic activity for improved bonding. The effects of varying fibre volume fractions (0–25% coconut fibre) on the mechanical properties were evaluated, with optimal compressive strength (2.89 MPa) obtained at 20 vol.% coconut fibre, while the optimum flexural strength and fracture toughness were obtained at 15 vol.% with values of 4.61 MPa and 1.23 MPa$\sqrt{m}$ respectively. Microstructural analysis by SEM revealed enhanced fibre-matrix interaction and reduced porosity. Comparisons with conventional sandcrete and fired clay bricks demonstrated that the optimized composite exhibited competitive performance. These findings demonstrate the potential for utilizing coconut fibre and RHA in sustainable brick production, offering improved mechanical performance while contributing to environmental sustainability and cost-effectiveness in building materials.

Keywords: Coconut fibre; Rice husk ash; Clay-cement composites; Mechanical properties; Sustainable building materials.

1. Introduction

The construction industry is undergoing a significant transformation towards sustainability by incorporating eco-friendly and sustainable materials in building application [1, 2]. Traditional construction materials like cement and bricks are associated with high energy consumption, significant carbon dioxide (CO_2) emissions, and depletion of non-renewable resources [3]. For instance, the production of Portland cement alone contributes approximately 7-8% of global CO_2 emissions, underscoring the urgent need for alternative, sustainable building materials [4]. Meanwhile, the use of composite materials that integrate agricultural waste such as rice husk ash (RHA) and natural fibres, like coconut fibre, offers a promising solution by reducing the environmental impact of construction activities while enhancing material properties.

Rice husk ash (RHA) is a well-known pozzolanic material widely recognized for its high silica content, which improves the mechanical and durability properties of cement-based composites [5]. The partial replacement of cement with RHA not only reduces the reliance on Portland cement but also mitigates the environmental problems associated with the disposal of rice husk, a major agricultural byproduct [6]. Previous studies [7, 8] have shown that RHA exhibits excellent pozzolanic reactivity due to its high surface area and amorphous silica content, leading to enhanced compressive strength and reduced permeability in concrete and mortar composites.

Natural fibres have gained significant attention as reinforcement materials in composite applications due to their availability, low cost, and superior mechanical properties, such as high tensile strength and toughness [9]. Coconut fibres, specifically, are known for their high lignin content, which provides better resistance to microbial degradation compared to other natural fibres, making them suitable for use in various environmental conditions [10]. The incorporation of RHA and coconut fibre into clay bricks has the potential to improve their mineralogical, textural, mechanical, and geotechnical properties, making them suitable for sustainable building applications. Clay, a natural material commonly used in brick production, has desirable properties such as plasticity, workability, and binding capacity [11]. The addition of RHA can alter the mineralogical composition of clay bricks, increasing the formation of secondary calcium silicate hydrates (C-S-H) that improve mechanical strength and durability. The presence of kaolinite, a dominant mineral phase in clay, contributes to its plasticity and ability to form strong interparticle bonds when mixed with pozzolanic materials like RHA [12]. The reinforcement with natural fibres can further enhance the toughness and impact resistance of clay bricks, leading to improved flexural and fracture toughness properties, which are crucial for non-load-bearing applications in

*Corresponding author. Email: kabiru.mustapha@kwasu.edu.ng

construction [13, 14].

From the literature summarized in Table 1, it is evident that several studies have independently investigated the use of RHA or natural fibres such as coconut fibre in enhancing the mechanical performance of clay- or cement-based materials. However, these studies often examined these additives in isolation, with limited understanding of the synergistic effects that could arise from their combined application in a clay–cement composite system. Furthermore, few works have correlated mineralogical and microstructural features with mechanical and geotechnical performance. Hence, the present study aims to bridge this gap by developing and characterizing composite clay–cement bricks reinforced with coconut fibre and RHA, with the goal of improving strength, thermal stability, and sustainability for construction applications.

Coconut fibre and rice husk ash (RHA) were selected as reinforcing and binding agents, respectively, due to their abundance, renewability, and proven enhancement of mechanical and durability properties in cementitious and clay-based materials. Nigeria produces over 2.1 million tons of coconuts and more than 4 million tons of rice annually, generating approximately 0.8 million tons of rice husk waste [20]. The improper disposal of these wastes contributes significantly to environmental pollution. The utilization of RHA, rich in reactive silica (typically 65–70%), has been shown to improve pozzolanic activity, increase strength, and reduce permeability in composite materials [21]. Similarly, coconut fibre possesses a tensile strength of 150–220 MPa and a modulus of elasticity between 4–6 GPa, making it suitable for reinforcing brittle matrices such as clay and cement composites [16]. Incorporating these agricultural wastes into brick production thus not only enhances performance but also promotes sustainable material development within tropical agricultural economies such as Nigeria and Southeast Asia.

The increasing demand for sustainable construction materials has led to growing interest in the utilization of agro-industrial waste in building applications. However, most existing studies have examined rice husk ash (RHA) and natural fibres such as coconut fibre independently in cementitious or clay matrices, focusing on their individual effects on mechanical and durability properties. Despite these advances, the combined influence of RHA and coconut fibre within a clay–cement composite system remains underexplored, particularly regarding their mineralogical, textural, and mechanical interactions. Bridging this gap is essential to understanding potential synergistic effects that can enhance the performance of sustainable composite bricks while reducing environmental waste and production costs.

Recent studies have focused on the development of sustainable composite bricks by incorporating agricultural wastes to achieve both economic and environmental benefits. For instance, research on composite bricks reinforced with natural fibres such as jute, sisal, and hemp, combined with pozzolanic materials, has demonstrated significant improvements in mechanical properties, including compressive and flexural strength, as well as enhanced thermal and acoustic insulation properties [22, 23, 24]. The utilization of RHA and coconut fibre in composite clay bricks not only leverages agricultural waste materials but also aligns with global sustainability goals by reducing CO_2 emissions, energy consumption, and waste generation during the production process.

The present study investigates the chemical, textural, mechanical, and geotechnical properties of composite clay-cement bricks reinforced with coconut fibre with the cement partially replaced with RHA. The aim is to evaluate the feasibility of using these eco-friendly composite materials for sustainable construction applications. Specifically, this study focuses on understanding how the incorporation of varying amounts of coconut fibre (0-25 vol.%) and RHA (20% of cement volume) affects the compressive strength, flexural strength, fracture toughness, and microstructural properties of the composite clay bricks. The findings of this research could provide valuable insights into the development of innovative, cost-effective, and environmentally sustainable building materials that are suitable for use in regions with abundant agricultural waste.

2. Materials and methods

2.1. Materials

The clay used in this study was sourced locally from Harmony Estate in the Akerebiata area of Ilorin, Kwara State, Nigeria. The claystone samples were collected from two different points approximately half a kilometre apart (Fig. 1). The sampling procedure involved fieldwork to locate and obtain representative samples of the clay. Fresh clay samples were dug from depths between 10 m and 15 m using a digger and shovel to ensure the collection of undisturbed material. Clay samples were collected at these depths to ensure retrieval of undisturbed, naturally consolidated clay unaffected by surface organic matter, weathering, and anthropogenic activities. Shallow deposits (<3 m) in the study area are typically mixed with topsoil and contain roots, organic impurities, and variable moisture content, whereas depths beyond 10 m provide more homogeneous, geologically stable clay layers suitable for engineering characterization [25]. The samples were carefully packed into labelled sample bags to prevent contamination. The selection of these clay deposits was based on their widespread availability and historical usage in the region for building and construction purposes. Previous studies have indicated that clays from the southwestern basement complex of Nigeria, including those from Akerebiata, have been utilized for brick production and other geotechnical applications [25, 26]. However, failures observed in some constructions necessitate further studies to enhance the mechanical and durability properties of these clay materials through reinforcement and stabilization.

Rice husk samples were sourced from milling sites within Ilorin, Kwara State, Nigeria and air-dried before undergoing calcination. The calcination process involved burning the husks in a traditional forge using coal as fuel, with moving air supplied via bellows to increase the temperature, resulting in highly pozzolanic rice husk ash (RHA) suitable for use in lime-pozzolana mixes and as a cement replacement [15]. The calcined husks were allowed to cool in a closed metal vessel for 24 hours, then sieved into fine powder (Fig. 2a). Coconut fibres were manually dehusked without water soaking to maintain an eco-friendly and low-cost approach. This method involved hand-pulling fresh husks from the hard shell, minimizing the cost and health risks associated with traditional methods (Fig. 2b).

2.2. Composite design and proportions

The composite clay bricks were prepared by partially replacing cement with RHA and reinforcing with coconut fibre at varying proportions. Sample designations S0–S5 correspond to composites reinforced with 0–25 vol.% coconut fibre, as presented in Table 2. Although the mix proportions are presented in volume percent (vol.%), the actual measurement and batching of coconut fibre were performed by converting the required volume fraction into an equivalent mass fraction. Coconut fibres have irregular geometry and natural variability in length and diameter, making direct volumetric measurement impractical and inconsistent. To ensure accuracy and repeatability, the bulk density of loosely packed coconut fibre was first determined (0.21 g/cm³), after which the target volume fraction for each mix was converted into mass using:

$$m_f = V_f \times \rho_{bulk} \quad (1)$$

Table 1: Summary of previous studies on natural fibre and RHA reinforced clay and cement composites.

Authors	Material composition	Key findings	Limitations
Oyekan & Kamiyo [15]	RHA as 10–30% partial replacement for cement	Improved pozzolanic reactivity and compressive strength up to 0% replacement	No reinforcement phase; only cementitious system studied
Mishra & Basu [16]	Coconut fibre in cement mortar (0–5 wt.%)	Enhanced toughness and crack resistance	No RHA inclun; limited microstructural correlation
Hafidh et al. [17]	Clay–cement composite with sawdust (0–30%)	Reduced density, improved thermal insulation	Weak mechanical strength due to poor matrix bonding
Singh et al. [18]	RHA in fired clay bricks (up to 0%)	Reduced bulk density and water absorption; optimal mechanical properties at 10–15% RHA	No fibre reinforcement considered; limited analysis of mineralogical changes
Rajapakse et al. [19]	Coconut fibre reinforced clay bricks (5–15%)	Improved tensile and flexural properties, reduced shrinkage	No pozzolanic additive; limited discusn on thermal stability

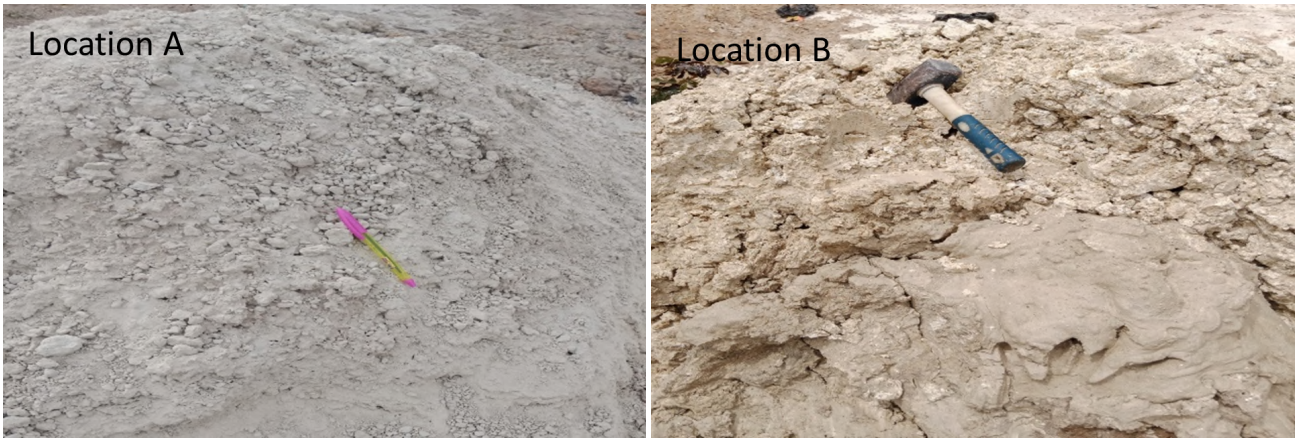

(a) Claystone sample from location A **(b)** Claystone sample from location B

Figure 1: Claystone sample from locations A and B.

where m_f is the mass of fibre required, V_f is the target volume fraction, and ρ_{bulk} is the measured bulk density of the fibre. This approach allowed precise and reproducible incorporation of fibre into the clay–cement–RHA matrix. The final mix ratios presented in Table 2 therefore reflect the intended volume fractions, while the actual batching was carried out using corresponding mass values to ensure consistency across all samples.

In this study, the clay fraction served as the primary matrix phase and therefore constituted the largest proportion in all mix designs. Although the clay content was not fixed, its proportion decreased only minimally as the coconut fibre content increased from 0 to 25 vol.% within the clay–fibre matrix. This approach ensured that clay remained the dominant phase controlling plasticity, compaction behaviour, and structural cohesion in the unfired composite bricks. The cement–RHA blend was intentionally fixed at 20 vol.% across all mixtures to maintain consistent pozzolanic contribution and binding action. Adjusting only the clay–fibre ratio allowed the study to isolate the direct influence of coconut fibre reinforcement while maintaining comparable binder chemistry and ensuring that the mechanical and microstructural performance differences arose from fibre variation rather than changes in cement or RHA content.

The clay, RHA, and coconut fibres were initially mixed in a dry state to ensure uniform distribution of the components. Water was then gradually added to the mixture to achieve the desired workability and consistency. The mixing was carried out using a mechanical mixer for 5 minutes to ensure a homogeneous blend. The prepared mixture was moulded into brick specimens using a standard mould. The moulds were compacted manually to achieve uniform density and reduce porosity. The bricks were then demoulded and cured under controlled conditions (relative humidity of 95% and temperature of 27 ± 2°C) for 28 days to allow adequate hydration and pozzolanic reactions to occur (Fig. 3). Although the composite contains cement, conventional water-curing was not adopted because the study aims to evaluate the performance of unfired, low-moisture, sustainable clay–cement composites. Furthermore, RHA, which is rich in amorphous silica (~67%), reacts pozzolanically with calcium hydroxide produced during cement hydration, contributing to additional strength gain over time. After compaction, samples were air-cured at ambient laboratory conditions (27–30°C) for 28 days. This curing regime aligns with previous studies on unfired clay–cement–pozzolan composites, where moisture retention within the clay matrix supports gradual hydration and pozzolanic reactions without external water curing. This approach also mirrors practical field conditions where unfired bricks are sun-dried rather than wet-cured.

Table 2: Composite design proportion.

Sample ID	RHA (Vol. %)	CEMENT (Vol. %)	Clay (Vol. %)	COCONUT FIBRE (Vol. %)	Total (Vol. %)
S0	4	16	80	0	100
S1	4	16	75	5	100
S2	4	16	70	10	100
S3	4	16	65	15	100
S4	4	16	60	20	100
S5	4	16	55	25	100

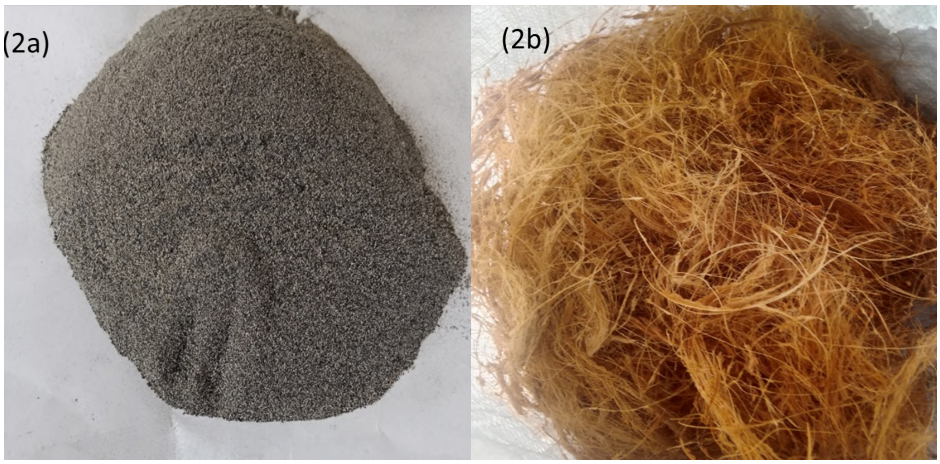

(a) Calcinated rice husk ash after sieving. **(b)** Dehusked coconut fibre.

Figure 2: Calcinated rice husk ash and dehusked cocnut fibre.

Figure 3: Moulded reinforced clay bricks.

2.3. Physical analysis

2.3.1. Particle size distribution

Hydrometer analysis was conducted to determine the proportions of clay, silt, and fine sand-sized particles within the samples. This analysis is essential because particle size distribution significantly influences the workability, compaction characteristics, plasticity, strength, and overall performance of unfired and stabilized clay bricks. Understanding the fines content also guides interpretation of geotechnical behaviour, including shrink–swell potential, permeability, and bonding within the composite matrix. Particle size distribution analysis was used to determine the percentage of different grain sizes within the soil sample. Information from the size distribution can be used to develop porosity and packing relationships. In this study, hydrometer analysis was used which involves sieving and sedimentation of a soil/water/dispersant suspension to separate particles, following Stoke's law [27]. The analysis utilized an ASTM 152H soil hydrometer, 1000 mL glass cylinders, a thermometer, an electric mixer, a weigh balance, and sieves. The dispersant solution was prepared by diluting 25% sodium hexametaphosphate in 900 mL of warm deionized water, cooling it, adding sodium carbonate to adjust the pH to 9, and diluting it to 1 L with deionized water [28]. Samples were weighed and sieved through 4.75 mm and 2 mm sieves, ensuring no aggregate particles remained on the sieve. A blank sample was prepared with 100 mL of 5% dispersing solution and 880 mL of deionized water, making up to 980 mL in a 1000 mL cylinder. Next, 50 g of the sieved soil sample was mixed with 100 mL of 5% dispersing solution for 60 seconds. The mixture was diluted to 1000 mL with deionized water and allowed to stand overnight for equilibration. After mixing with a plunger for 30 seconds, the temperature and hydrometer readings were taken at 40 seconds (to measure silt and clay in suspension) and at 6 hours (to measure clay after silt had settled). To determine the sand content, the cylinder contents were washed thoroughly and passed through a 0.20 mm sieve. Particles retained on the sieve represented the coarse sand fraction, which was transferred to a pre-weighed pan, dried in an oven at 110°C, cooled in a desiccator, and then weighed. The percentages of clay, silt, and sand were calculated using the following formulas:

$$\%Clay = \frac{R_{6hr} \times 100}{W_s} \tag{2}$$

$$\%Slit = \frac{R_{40sec} \times 100}{W_s} - \%Clay \tag{3}$$

$$\%Sand = 100 - \%Clay - \%Slit \tag{4}$$

Where: R_{6hr}= corrected hydrometer reading at 6 hours, R_{40sec}= corrected hydrometer reading at 40 seconds and W_s= mass of oven-dry soil sample

2.3.2. pH analysis and cation exchange capacity

The pH of clay soil indicates its acidity or alkalinity, which can range from acidic to slightly alkaline depending on parent materials or environmental conditions. In this study, the pH of clay soil samples was measured using a pH meter. To prepare, 5 g of ground clay soil was weighed into a beaker, and 100 mL of distilled water was added. The mixture was agitated for 30 minutes in a water bath shaker, allowed to settle by sedimentation, and then filtered to separate the water from the soil sediment. The pH meter was calibrated using buffer solutions of 4.00, 9.18, and 6.86 before inserting the electrode into the filtered water. Readings were allowed to stabilize, and the procedure was repeated three times to obtain an average pH value.

The cation exchange capacity (CEC) of soil is a critical property that indicates its ability to hold and exchange positively charged ions, such as magnesium, calcium, potassium, and sodium, which are essential soil nutrients. A higher CEC reflects a greater capacity for nutrient retention and soil fertility due to the increased negative charge and ability to hold more cations. To determine the CEC, 5g of ground clay soil was digested by mixing with 5 mL of hydrochloric acid and 10 mL of sulfuric acid in a beaker, followed by heating on an electric heater for 10-15 minutes. The mixture was then cooled, diluted with 50 mL of distilled water, and filtered.

The acidity and alkalinity of the solution were determined using a pH meter. The resulting solution was analysed for exchangeable cations using Atomic Absorption Spectroscopy (AAS) at the University of Ilorin, Nigeria Central Research Laboratory.

2.3.3. Conductivity and salinity analysis

Electrical conductivity (EC) measures how well clay soil can conduct electricity, reflecting the concentration of dissolved salts. Clay soil generally has lower EC compared to sandy soil due to their high cation exchange capacity, which retains cations and reduces free ions available for conduction. Salinity, representing the concentration of soluble salts, can cause efflorescence in bricks, affecting both appearance and structural integrity. The analysis of conductivity and salinity was conducted at the Integrated Research Laboratory, Ilorin, Nigeria using a multiparameter instrument. Salinity was measured in parts per million (ppm) and converted to decisiemens per meter (dS/m) using the conversion factor 1 dS/m ≈ 640 ppm, with the formula:

$$\frac{ds}{m} = \frac{ppm}{640} \tag{5}$$

2.4. Mineralogical composition analysis

2.4.1. X-ray diffraction (XRD) analysis

X-ray Diffraction (XRD) analysis was utilized to determine the mineralogical composition of the rice husk ash (RHA)/clay mixtures. The analysis was conducted using a Rigaku D/Max-IIIC X-ray diffractometer at Rolab Research and Diagnostic Laboratory in Ibadan, Nigeria. Samples were prepared, mounted on a rotating stage, and analyzed using $\theta - \theta$ settings with a 2θ range from 2 to 50 degrees, a step size of 0.065 degrees, and a scanning rate of 2 degrees per minute, utilizing CUKA radiation at 40 kV and 20 mA. Mineralogical compositions were estimated based on peak intensities and compared with standard data from the ICDD database.

2.4.2. Thermogravimetric analysis of composite samples (TGA)

Thermogravimetric Analysis (TGA) were performed on the composite samples to study their thermal stability and phase transitions. TGA measures the change in mass of a sample as a function of temperature in a controlled environment, such as air or nitrogen, providing insights into thermal decomposition and absorption. In this study, dynamic thermogravimetry was used, where the sample was heated at a varying temperature rate. Approximately 5 grams of each sample was weighed and placed in the analysis chamber, and the nitrogen gas flow rate was set to 20 psi. The TGA4000 model was utilized at the National Steel Raw Materials Exploration Agency in Kaduna, Nigeria with weight changes recorded as a function of temperature over time and presented graphically.

2.4.3. X-ray fluorescence (XRF) spectrometer

X-ray fluorescence (XRF) spectrometry was employed to analyse the qualitative and quantitative elemental composition of clay particles, rice husk ash and cement. This non-destructive technique uses wavelength-dispersive spectroscopic principles to measure both major and trace elements in samples such as rocks, sediments, and fluids. The samples were dried and prepared to achieve a homogenous particle size distribution before analysis. During the XRF process, the samples were exposed to a primary X-ray source, and the emitted secondary X-rays were measured to determine the elemental composition.

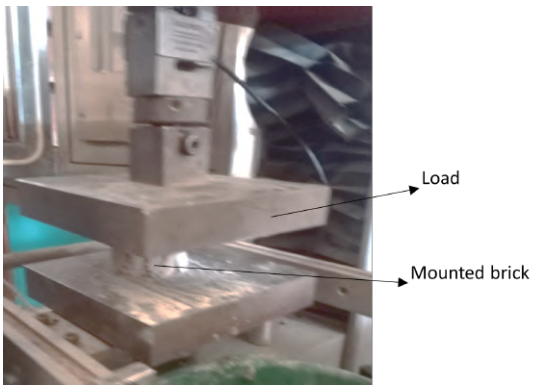

Figure 4: Testometric FS 50 AT testing machine mounted with compressive strength accessories.

2.5. Mechanical analysis of composite samples

2.5.1. Compressive strength analysis

The compressive strength of the composite samples was evaluated to determine their ability to resist compressive stress before failure, following ASTM C39 [29]. This test is crucial for assessing the safety and durability of materials used in construction. The Clay-Cement-RHA reinforced samples, prepared with varying compositions, were tested using a 5000 kN digital compression machine (Testometric FS 50 AT). Cylindrical samples with dimensions of 60 mm in diameter and 60 mm in height were subjected to gradually increasing load until failure (Fig. 4). A total of 36 samples (6 per composition level) were tested, and the compressive strength (σ) was calculated using equation 6.

$$\sigma = \frac{F}{A} \tag{6}$$

where F is the average maximum force and A is the cross-sectional area of the sample.

2.5.2. Flexural analysis of composite samples

The flexural strength of the composite samples was tested using the three-point bending method on rectangular samples measuring 200 mm in length, 20 mm in thickness, and 30 mm in width (Fig. 5). The tests were conducted on a Testometric FS 50 AT testing machine at the University of Ilorin, Nigeria. Each sample was clamped between grips, and a load was gradually applied until fracture occurred. A total of 36 samples were tested across different reinforcement levels, ranging from 0% to 25%. The average flexural strength (σ_f) for four samples at each reinforcement level was calculated using equation 7 [30], with F as the average maximum load, L as the span length (160 mm), H as the sample thickness (20 mm), and B as the width (30 mm).

$$\sigma_f = \frac{3FL}{2BH^2} \tag{7}$$

2.5.3. Fracture toughness of composite samples

The fracture toughness of the composite samples was assessed using a single edge-notched bending (SENB) test approach, where specimens were notched at the centre to a crack length of 6 mm, corresponding to a crack-width ratio (a/w) of ~ 0.3. Precracked samples were tested on a Testometric FS 50 AT testing machine. The fracture toughness K_{IC} was calculated using equations 8 and 9 [30], based on the compliance function $f(\frac{a}{w})$, flexural stress σ_f, and crack length a, following standards outlined in ASTM E399 [31].

$$K_{IC} = f(\frac{a}{w})\sigma_f\sqrt{\pi a} \tag{8}$$

Figure 5: Testometric FS 50 AT testing machine with flexural sample mounted on it.

$$F(\frac{a}{w}) = \frac{3(\frac{a}{w})^{\frac{1}{2}}}{2(1+2\frac{a}{w})(1-\frac{a}{w})^{\frac{3}{2}}} \times [1.99 - (\frac{a}{w})(1-\frac{a}{w}) \times (2.15 - 3.93\frac{a}{w} + 2.7\frac{a^2}{w^2})] \quad (9)$$

2.6. Microstructural characterization of composite samples

The microstructure of the composite samples was characterized using Scanning Electron Microscopy (SEM) combined with Energy Dispersive X-Ray Spectrometry (EDS) at Spectromass Laboratory, Kaduna, Nigeria. The SEM provides detailed microstructural information of sample surfaces by discharging an electron beam through an electron gun, which interacts with the sample surface to generate signals. A Carl Zeiss MA-10 Scanning Electron Microscope running at 15 kV accelerating voltage was used to examine the samples' microstructure. The SEM data offers a comprehensive understanding of the composites' properties as displayed in a two-dimensional spatial variation image.

3. Results and discussion

3.1. Particle size distribution

Table 3: Particle size distribution analysis.

Sample	Location A &B (%)
Coarse Sand	45.95
Fine	52
Clay	25.05
Silt	29.00
Sand	45.95
Colour	Dirty white

The Particle Size Distribution (PSD) analysis of the clay sand from Harmony Estate in the Akerebiata area of Ilorin, Nigeria presented in Table 3 reveals that the samples are primarily silty clays, composed of 45.95% coarse sand, 25.05% clay, and 29.00% silt, indicating a higher content of fine particles than coarse ones. The sand fraction, determined by washing the sample for 6 hours and sieving through a 0.20 mm mesh, confirms the absence of gravel, with the coarse sand particles retained on the sieve. The clay and silt percentages were calculated by correcting hydrometer readings at 6 hours and 40 seconds, respectively, revealing significant silty and clayey components. The particle size composition, along with the dirty white colour of the samples can potentially influence the material's plasticity and workability for brick-making applications.

3.2. pH analysis and cation exchange capacity

The pH of the clay sand measured at 7.0 (Table 4), which is neutral, falls within the ideal range of 6.8 to 8.0 recommended for brick-making materials to ensure stability, durability, and chemical compatibility with construction mortar. This neutral pH is particularly advantageous because it minimizes the risk of corrosion for metal reinforcements and ensures compatibility with alkaline mortars, which are commonly used in construction [32]. Furthermore, the neutral pH supports the structural integrity and longevity of the final brick product by preventing detrimental chemical reactions that might otherwise weaken the brick over time, contributing to overall material performance and durability [33].

Table 4 also presents the cation exchange capacity (CEC) of the clay sand, measured at 1.04 cmol/kg with exchangeable elements ranging from 0.10 cmol/kg for sodium (Na) and magnesium (Mg) to 0.2 cmol/kg for potassium (K), indicates a modest ability to retain and exchange cations, which suggests limited active sites for interacting with other materials. This low CEC, attributed to the dominance of kaolin as revealed by XRD analysis and the low content of alkali and alkaline earth metals shown by XRF analysis, implies reduced plasticity and binding strength, potentially leading to less robust bricks. However, it may reduce shrinkage and cracking during drying, easing the moulding process. Consequently, while the clay's low CEC may affect brick strength, it could offer advantages in manufacturing by minimizing drying defects and simplifying water management.

3.3. Conductivity and salinity analysis

The conductivity of the clay sand measured at 0.47 ds/m and its salinity at 0.047 ds/m indicates low levels of dissolved salts, which are beneficial for brick making. Low salinity makes clay easier to mould and shape while reducing the risk of efflorescence, which can lead to unsightly white deposits on brick surfaces. The low conductivity also minimizes the risk of corrosion when the bricks encounter metal reinforcements, enhancing the long-term stability and durability of structures [34]. Additionally, these low values help prevent salt deposits during the drying process, contributing to a smoother and more aesthetically pleasing brick finish.

3.4. X-ray diffraction analysis of clay mixture

The X-ray Diffraction (XRD) analysis of the clay mixture, as shown in Fig. 6, reveals that kaolinite is the dominant mineral, as indicated by prominent peaks at 2θ values of 13°, 23°, 25°, and 63°. Other minerals identified include quartz, illite, muscovite, dolomite, calcite, and microcline. The high-intensity kaolinite peaks indicate their well-defined crystalline structure, consisting of alternating tetrahedral and octahedral layers. However, the addition of rice husk ash (RHA), rich in amorphous silica, and the organic nature of coconut fibres have introduced amorphous components to the material, as shown by broader, less-defined peaks in the XRD pattern. These semi-crystalline features align with findings in similar studies [35, 36]. The overall structure is a mix of crystalline clay and non-clay minerals, enhanced by amorphous phases from RHA and fibre reinforcements.

3.5. Thermal stability analysis of the natural fibre reinforced composite clay bricks

The thermal stability analysis of natural fibre-reinforced composite clay bricks, assessed using Thermogravimetric Analysis (TGA), reveals distinct mass loss events across all samples, primarily occurring between 300°C and 500°C, accounting for over 60% of the total mass loss (Fig. 7).

The thermogravimetric analysis (TGA) revealed three major mass-loss stages across all composite samples, each corresponding

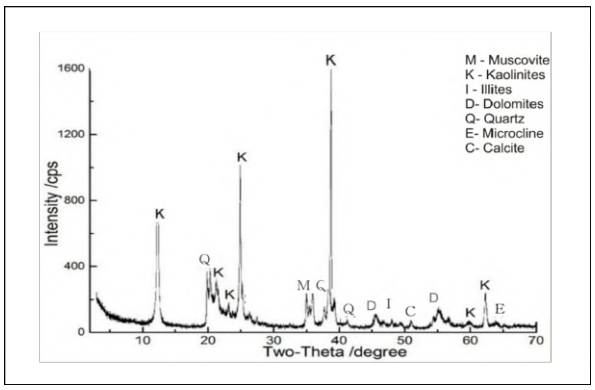

Figure 6: XRD analysis of clay/RHA mixture

to specific thermal degradation events. In the first stage (25–350 °C), samples exhibited 8–12% mass loss, primarily due to evaporation of physically bound moisture and dehydration of surface and pore water. The second stage occurred between 350–500 °C, where a significant 28–35% mass loss was recorded, representing the decomposition of organic constituents, including the coconut fibre, and the dehydroxylation of clay minerals. This stage accounted for the largest proportion of total degradation, confirming that fibre-rich samples show more pronounced weight loss. The third stage (500–800 °C) produced an additional 40–48% mass loss, attributed to the breakdown of residual organics and mineral phases such as carbonates. Notably, samples containing 10–20 vol.% fibre demonstrated lower total mass losses (82–85%) compared to both the control sample and the 25 vol.% fibre composites, indicating improved thermal stability at intermediate fibre contents. Conversely, the 25 vol.% sample recorded a total mass loss of about 91%, like the unreinforced clay–cement matrix, suggesting that excessive fibre addition compromises the thermal integrity of the composite. These quantitative trends confirm that 10–20 vol.% coconut fibre provides the most favourable balance between organic decomposition and matrix stability, supporting the mechanical performance trends observed in the study.

3.6. X-ray fluorescence (XRF) analysis of clay and RHA Samples

The major oxide analysis shows that clay samples from Locations A and B, as well as the Rice Husk Ash (RHA), show significant variation in oxide concentrations. SiO_2 is highest in RHA at 66.95%, indicating RHA's potential for pozzolanic activity (Table 5). Clay sample from Location A has a higher Al_2O_3 content (20.16%) compared to Location B (12.30%). Notably, Location B contains a high amount of MnO (10.01%), which is nearly absent in Location A. RHA also contains considerable amounts of CaO (5.50%) and K_2O (5.20%) compared to the clays. These differences suggest varying mineralogical properties, with RHA showing higher potential as a supplementary cementitious material due to its high silica content.

Table 6 shows the chemical comparison between Rice Husk Ash (RHA) and Portland Cement. This shows that RHA is highly rich in silica (SiO_2) with 66.95%, significantly higher than the 22.07% in Portland Cement. This high silica content makes RHA a promising pozzolanic material that can improve the strength and durability of cement-based composites [37]. On the other hand, Portland Cement is predominantly composed of calcium oxide (CaO) at 65.44%, which is essential for the cement's hydraulic properties. RHA also contains notable amounts of alumina (Al_2O_3) and iron oxide (Fe_2O_3), which contribute to its pozzolanic activity, while its lower lime (CaO) content may result in a slower setting rate compared to Portland Cement. The analysis underscores the potential of RHA as a supplementary cementitious material that can partially replace Portland Cement, reducing reliance on traditional cement and contributing to sustainability in construction.

3.7. Microstructural characterization of composite sample

The SEM micrographs of composite samples are presented in Fig. 8. For sample S0 (0 vol.% fibre in Fig. 8a, the microstructure shows a porous and non-homogeneous matrix, which may explain the lower mechanical properties. Sample S1 (5 vol.% fibre) in Fig. 8b shows a slight improvement in fibre distribution, but the matrix still exhibits significant voids and non-uniform particle distribution. The SEM micrograph of sample S2 (10 vol.% fibre) in Fig. 8c reveals better fibre dispersion with reduced pore sizes, contributing to improved load-bearing capacity. For sample S3 (15 vol.% fibre) in Fig. 8d, a more compact and homogeneous matrix is evident, with enhanced fibre-matrix bonding, corresponding to the optimum flexural strength and fracture toughness observed. However, for sample S4 containing 20 vol.% fibre (Fig. 8e), the matrix shows even denser packing and fewer voids, explaining the optimum compressive strength obtained at this volume fraction. Finally, sample S5 (25 vol.% fibre) presented in Fig. 8f shows excessive fibre content, leading to agglomeration and non-uniformity, which negatively affects mechanical performance due to stress concentration and poor matrix continuity.

These observations align with the mechanical test results, where 20 vol.% fibre yielded the highest compressive strength due to the dense matrix structure, while 15 vol.% fibre exhibited the best flexural strength and fracture toughness due to optimal fibre-matrix interaction and dispersion. Beyond 20 vol.%, excessive fibre loading compromises the integrity of the matrix, reducing mechanical properties.

3.8. Compressive strength of composite samples

The compressive strength results for fibre-reinforced composites, as shown in Fig. 9a and 9b, demonstrate a gradual increase with fibre content up to 20 vol.%, followed by a reduction at 25 vol.%. Sample S4 (20 vol.% fibre) exhibited the optimum compressive strength, where the material achieves its highest mechanical performance. This improvement can be attributed to the ability of fibres to bridge micro-cracks and distribute stress effectively across the matrix, enhancing load-bearing capacity. The SEM images for samples S3 and S4 support this by showing well-embedded fibres, reduced porosity, and uniform fibre distribution, all of which contribute to the observed increase in strength.

Although Fig. 9a and 9b appear visually similar, they serve distinct analytical purposes. Fig. 9a presents the compressive strength of the composite bricks as a function of fibre volume fraction only, enabling direct evaluation of how coconut fibre affects load-bearing capacity. In contrast, Fig. 9b compares the optimum composite strength with benchmark values for conventional sandcrete and fired clay bricks, providing context for assessing the material's practical performance in relation to commonly used masonry units. The compressive strength tests were conducted in accordance with ASTM C39, a widely adopted standard for cementitious materials, which ensures consistency in loading rate, specimen preparation, and failure assessment. This alignment with an established code validates the measurements and enables meaningful comparison with existing masonry standards, which generally require compressive strengths in the range of 2.5–3.5 MPa for non-load-bearing units. Minimum compressive-strength requirements for common masonry units vary by standard and region; for example, the Nigerian Industrial Standard for sandcrete blocks (NIS 87:2007) specifies minimum compressive strength values (typically ≈ 2.5 N/mm², with higher classes up to ~3.45 N/mm² depending on block class) [38]. The comparative analysis therefore demonstrates that the developed composite bricks, particularly at 15–20 vol.% fi-

Table 4: CEC results of the clay sand.

Element (Cmol/kg)	Potassium (K)	Calcium (Ca)	Magnesium (Mg)	Sodium (Na)	pH	CEC (Cmol/kg)
Exchangeable cation	0.20	0.17	0.10	0.10	7.0	1.04

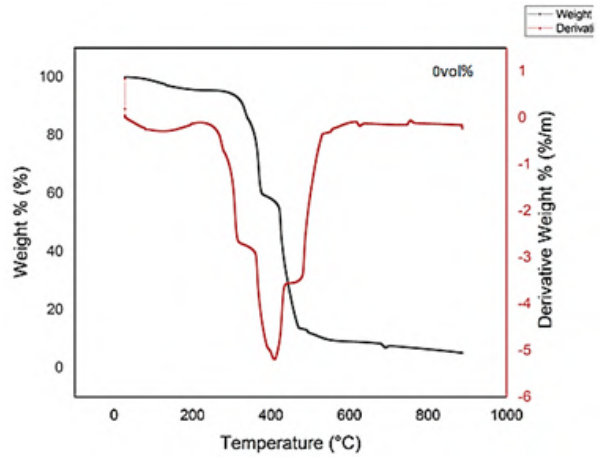

(a) TGA analysis of composite sample containing 0 vol.

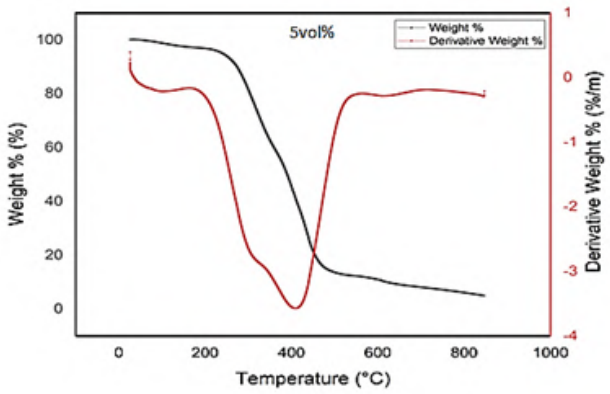

(b) TGA analysis of composite sample containing 5 vol.

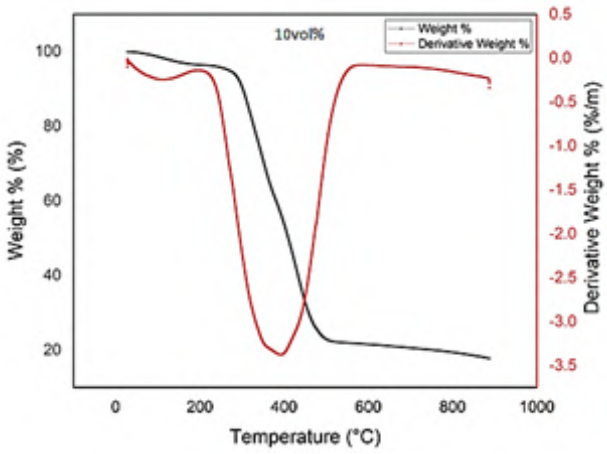

(c) TGA analysis of composite sample containing 10 vol.

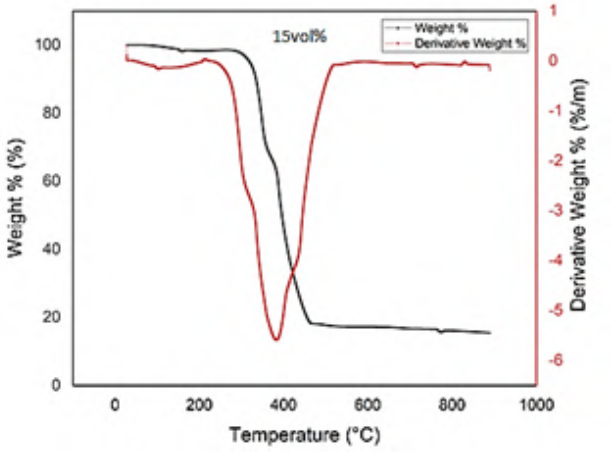

(d) TGA analysis of composite sample containing 15 vol.

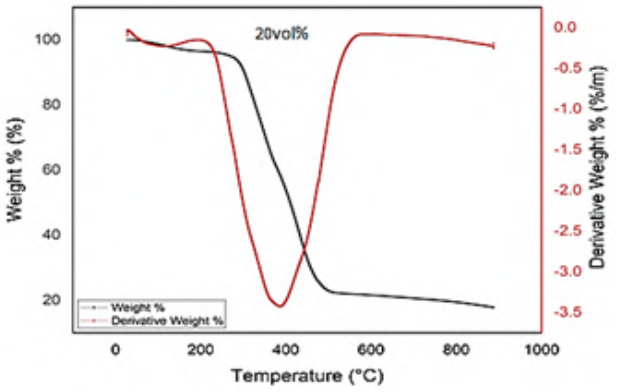

(e) TGA analysis of composite sample containing 20 vol.

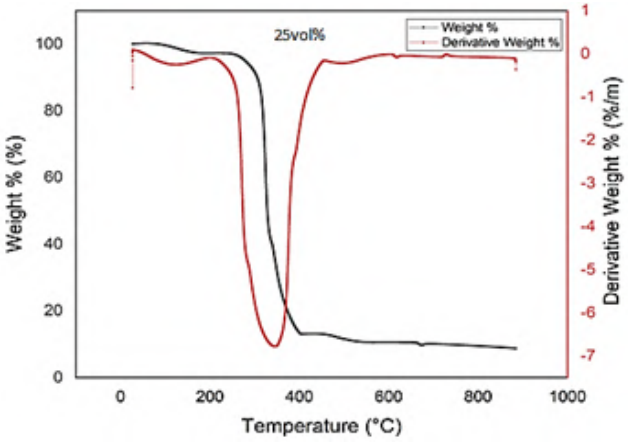

(f) TGA analysis of composite sample containing 25 vol.

Figure 7: TGA analysis of composite sample.

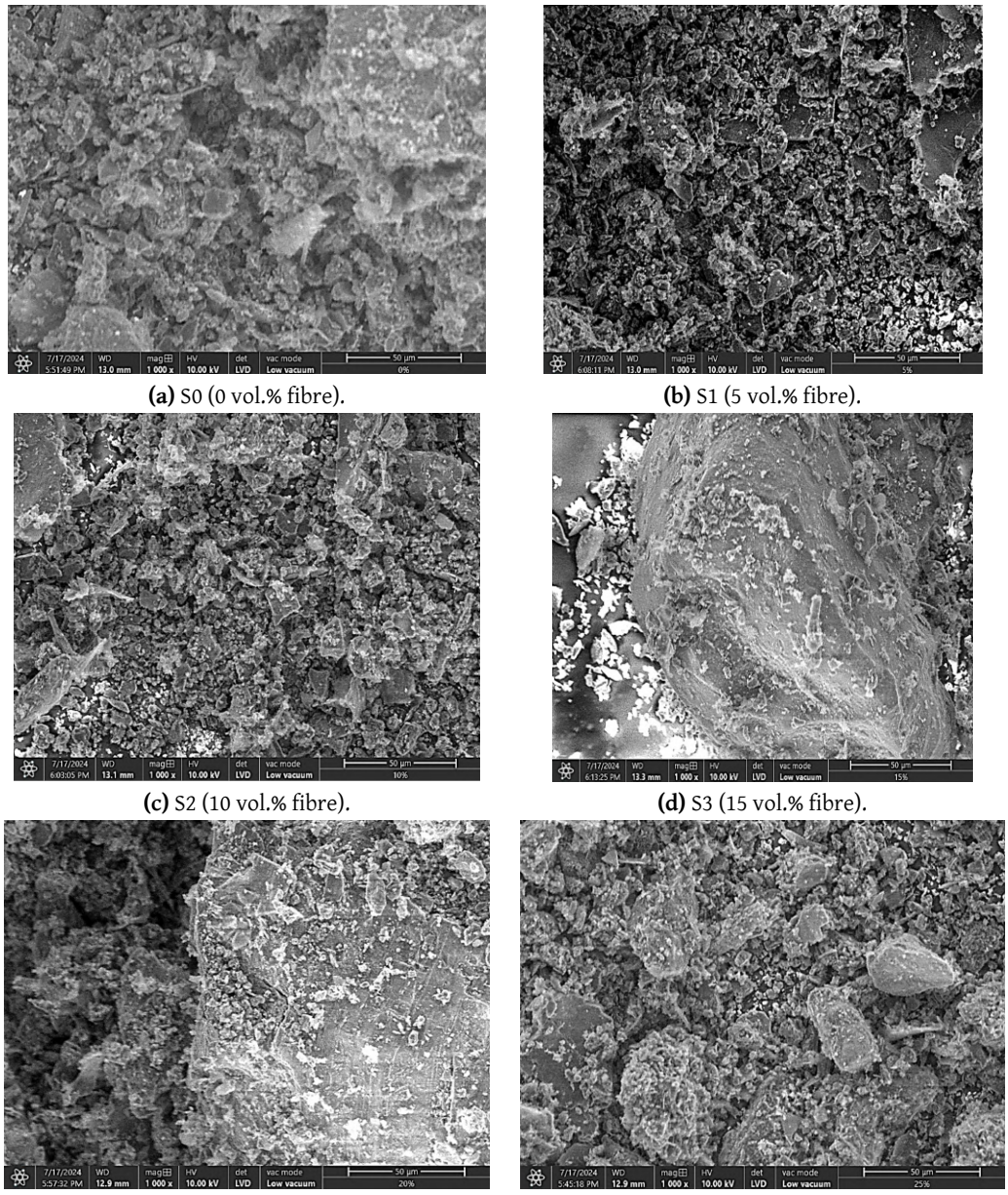

(a) S0 (0 vol.% fibre). **(b)** S1 (5 vol.% fibre).

(c) S2 (10 vol.% fibre). **(d)** S3 (15 vol.% fibre).

(e) S4 (20 vol.% fibre). **(f)** S5 (25 vol.% fibre).

Figure 8: SEM images of composites samples.

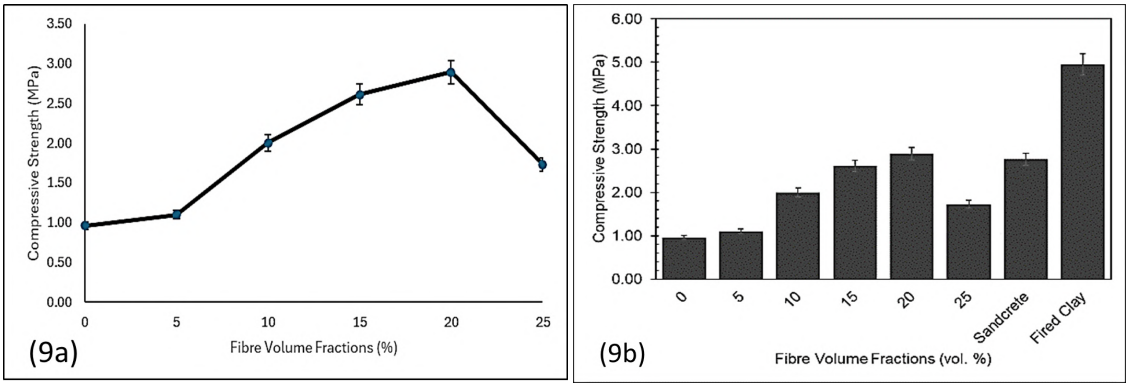

(a) Compressive strength of composite bricks as a function of fibre volume fraction. **(b)** Comparison of composite compressive strength with conventional sandcrete and fired clay bricks.

Figure 9: Compressive Strengths of composite samples

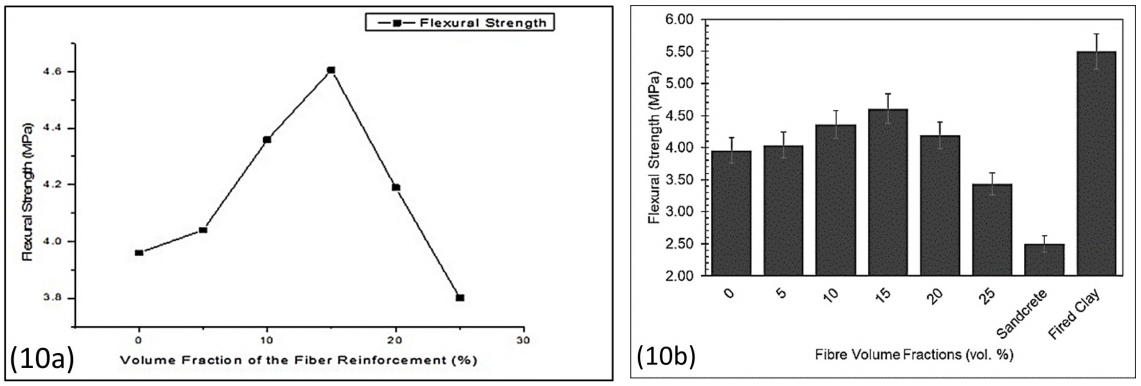

(a) Flexural strength of composite bricks as a function of fibre volume fraction. **(b)** Comparison of composite flexural strength with conventional sandcrete and fired clay bricks.

Figure 10: Flexural Strengths of composite samples.

Table 5: Concentrations of major oxides in the materials.

OXIDES	Clay (Location A)	Clay (Location B)	RHA
SiO_2	58.20	63.30	66.95
AI_2O_3	20.16	12.30	6.50
Fe_2O_3	1.30	2.15	5.70
TiO_2	2.04	0.20	0.50
CaO	2.33	1.40	5.50
K_2O	2.04	0.30	5.20
Na_2O	0.15	3.70	0.17
MgO	1.95	0.55	3.24
MnO	0.01	10.01	0.02
P_2O_5	0.45	1.05	3.70
SO_3	0.25	3.02	-
LOI	10.80	2.02	-
SUM	99.68	100	97.48

Table 6: Chemical analysis of cement and rice husk ash compared to ordinary portland cement.

Major Oxide	Rice Husk Ash (RHA)	Portland Cement
SiO_2	66.95	22.07
AI_2O_3	6.50	5.34
Fe_2O_3	5.70	2.47
TiO_2	0.50	-
CaO	5.50	65.44
K_2O	5.20	-
Na_2O	0.17	0.75
MgO	3.24	3.79
MnO	0.02	-
P_2O_5	3.70	-
SO_3	-	2.87

bre content, fall within the acceptable range of standard brick performance.

3.9. Flexural strength of composite samples

The flexural strength of the fibre-reinforced clay-cement-RHA composites increases with the fibre volume fraction up to 15 vol.% (Sample S3), reaching a peak value of 4.61 MPa as shown in Fig. 10a. This improvement can be attributed to the enhanced fibre-matrix interaction, which helps in stress transfer during bending. Beyond 15 vol.%, the flexural strength began to decline, likely due to fibre agglomeration and non-uniform distribution, which weakened the overall structure by introducing stress concentration points. The composite with 25 vol.% of fibre exhibited a lower flexural strength of 3.89 MPa, indicating that excess fibre content leads to a detrimental effect on the mechanical performance of the material.

The decline in flexural strength observed at 20 vol.% coconut fibre, despite the earlier improvement at 15 vol.%, is consistent with fibre-reinforced composite behaviour reported in similar studies. Excessive fibre loading tends to introduce fibre agglomeration, create weak interfacial zones, and increase porosity, all of which impair stress transfer efficiency across the matrix. Published works on natural-fibre-reinforced earth and cementitious composites have similarly reported strength reduction at high fibre dosages due to poor fibre dispersion and the development of micro-voids that act as crack-initiating sites [39, 40]. The SEM images in this study support these findings. While 15 vol.% fibre produced a well-distributed network that bridged microcracks and enhanced bending performance, the 20 vol.% sample exhibited fibre clustering and larger voids, reducing matrix continuity and compromising load transfer during bending. Thus, the optimal flexural performance at 15 vol.% corresponds to a balance between matrix integrity and effective fibre reinforcement. Fig. 10a and 10b serve two complementary roles: Fig. 10a illustrates the influence of fibre addition on flexural behaviour and helps identify the optimum dosage, while Fig. 10b compares the developed composite with conventional brick units to demonstrate its improved performance and suitability for non-load-bearing structural applications.

When compared with conventional bricks such as sandcrete and fired clay as shown in Fig. 10b, the fibre-reinforced composites exhibit superior performance, especially at 15 vol.% fibre, which outperforms sandcrete and is only slightly lower than fired clay bricks. The significant difference in flexural strength between sandcrete (2.90 MPa) and fired clay (5.40 MPa) is due to the inherent mechanical properties of the clay and firing process, which contribute to higher structural integrity. The introduction of natural fibres into the clay-cement-RHA matrix offers an eco-friendly alternative that significantly enhances mechanical properties compared to traditional sandcrete while maintaining competitive performance relative to fired clay.

3.10. Fracture toughness of composite samples

The fracture toughness results for the fibre-reinforced composites, as seen in Fig. 11a, shows an increase in toughness with increasing fibre volume fraction up to 15 vol. %, reaching a peak

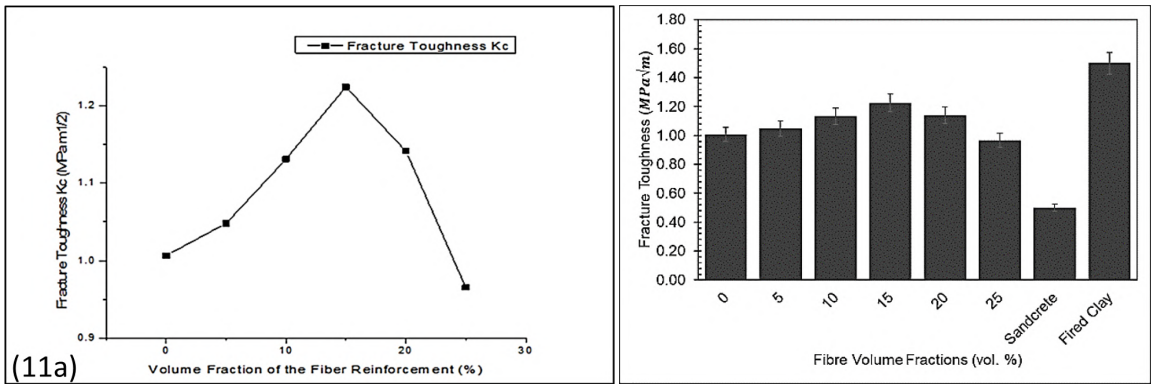

(a) Fracture toughness of composite bricks as a function of fibre volume fraction. **(b)** Comparison of composite fracture toughness with conventional sandcrete and fired clay bricks.

Figure 11: Fracture Toughness of composite samples.

value of approximately 1.23 MPa√m (Sample S3). This trend suggests enhanced crack resistance at optimal fibre content due to better fibre-matrix bonding and energy dissipation mechanisms. Beyond 15 vol.%, the fracture toughness decreases, likely due to fibre agglomeration and poor dispersion, which create weak points in the matrix that facilitate crack initiation and propagation.

When compared to conventional building materials (Fig. 11b), the reinforced composites show superior fracture toughness compared to sandcrete, which exhibits a much lower value around 0.5 MPa√m. However, the fracture toughness of fired clay bricks surpasses all the composites, suggesting that traditional fired clay still provides excellent toughness due to its high density and low porosity. Nonetheless, the composites' performance demonstrates the potential of using agricultural waste fibres in producing sustainable and relatively tough building materials.

The variation in optimum performance across different fibre contents can be attributed to contrasting reinforcement mechanisms governing compressive versus tensile-related behaviour. The flexural strength and fracture toughness peaked at 15 vol.% fibre due to effective crack bridging, uniform fibre dispersion, and strong fibre–matrix interfacial bonding observed in the SEM micrographs, where fibres were well aligned within the matrix with minimal pull-outs. At this fibre content, reinforcement primarily improved resistance to crack initiation and propagation, which governs tensile-dominated failure [41]. Conversely, compressive strength peaked at 20 vol.% fibre because the additional fibre content contributed to improved energy absorption and internal reinforcement under axial loading, despite the onset of local fibre clustering [30]. However, at ≥20 vol.% fibre, SEM analysis revealed significant fibre agglomeration, interfacial gaps, and increased porosity, leading to lower flexural and toughness values as load transfer pathways were disrupted. This shows that moderate fibre content enhances tensile performance by promoting uniform reinforcement, whereas higher contents favour compressive resistance until the point where matrix cohesion deteriorates due to excessive fibre inclusion.

4. Conclusion

1. This study developed and characterized sustainable clay–cement composite bricks reinforced with coconut fibre and cement partially substituted with rice husk ash (RHA), with fibre contents varying from 0–25 vol.%.

2. The composite system incorporates coconut fibre as the primary reinforcement, while rice husk ash functions solely as a pozzolanic material for partial replacement of cement. Physical and chemical characterization of the clay confirmed a kaolinitic composition with high silica content (58.20–63.30%) and moderate alumina (12.30–20.16%), while RHA contained 66.95% amorphous SiO_2, supporting its suitability as a pozzolanic cement replacement. The clay exhibited a neutral pH (7.0), low salinity (0.047 dS/m), low CEC (1.04 cmol/kg), and fine-dominated particle structure (25.05% clay, 29.00% silt), indicating reduced shrinkage tendencies but moderate binding capability.

3. Mechanical performance showed that compressive strength increased from 0.95 MPa (0 vol.%) to a maximum of 2.89 MPa at 20 vol.% fibre reinforcement, meeting the requirements for non-load-bearing masonry units. Flexural strength and fracture toughness peaked at 4.61 MPa and 1.23 MPa√m, respectively, at 15 vol.% fibre, demonstrating enhanced crack bridging and improved resistance to brittle failure at moderate fibre content. At higher fibre loadings (≥20 vol.%), mechanical performance declined due to agglomeration and increased porosity, confirming that excessive fibre disrupts matrix cohesion.

4. Thermal analysis showed improved thermal stability between 10–20 vol.% fibre, with mass loss reduced from 95.13% (5 vol.%) to 83.54% (20 vol.%) up to 900 °C. SEM microstructural observations confirmed improved fibre–matrix bonding and reduced pore dispersion at ≤20 vol.% fibre, while higher proportions exhibited clustering and pull-outs consistent with mechanical degradation.

5. Overall, optimal mechanical and thermal performance occurs at fibre contents between 15–20 vol.%, depending on property of interest. These findings demonstrate that combining coconut fibre with RHA-modified clay–cement systems produce an unfired, low-carbon brick suitable for sustainable housing applications, particularly in regions with abundant agricultural waste resources.

6. While the study demonstrates clear performance improvements at optimum fibre contents, the findings are limited to untreated fibres and laboratory-controlled compaction without durability evaluation. The moderate compressive strength values indicate the material is best suited for non-load-bearing applications, and further optimization such as fibre surface treatment, controlled densification techniques, and supplementary binders may be required to expand use to structural applications.

7. Future studies should also assess long-term durability under moisture cycling, biodegradation, and environmental exposure, as well as perform scale-up to support industrial adoption.

Acknowledgment

The authors gratefully acknowledge the support by the Federal Government of Nigeria through the TETFund Institution-Based Research (IBR) program for providing the financial support for this study under the allocation KWA-SUIBR/CRIT/270921/VOL1/TETF2020/0010.

References

[1] Singh C S, Green construction: Analysis on green and sustainable building techniques, *Civil Engineering Research Journal*, 4(3). ISSN 2575-8950. https://doi.org/10.19080/cerj.2018.04.555638.

[2] Shehata N, Mohamed O A, Sayed E T, Abdelkareem M A & Olabi A G, Geopolymer concrete as green building materials: Recent applications, sustainable development and circular economy potentials, *Science of The Total Environment*, 836 (2022) 155577. ISSN 0048-9697. https://doi.org/10.1016/j.scitotenv.2022.155577.

[3] Ajayi O O, Ngene B U & Ogbiye S A, Assessment of the spatial distribution of carbondioxide pollution emitted by cement industry located in Sagamu, Nigeria, 1054(1) (2022) 012048. ISSN 1755-1315. https://doi.org/10.1088/1755-1315/1054/1/012048.

[4] Andrew R M, Global CO2 emissions from cement production, 1928-2018, 11(4) (2019) 1675–1710. ISSN 1866-3516. https://doi.org/10.5194/essd-11-1675-2019.

[5] Msinjili N S, Schmidt W, Rogge A & Kühne H C, Rice husk ash as a sustainable supplementary cementitious material for improved concrete properties, *African Journal of Science, Technology, Innovation and Development*, 11(4) (2019) 417–425. ISSN 2042-1346. https://doi.org/10.1080/20421338.2018.1513895.

[6] Celik K, Jackson M, Mancio M, Meral C, Emwas A H, Mehta P & Monteiro P, High-volume natural volcanic pozzolan and limestone powder as partial replacements for portland cement in self-compacting and sustainable concrete, *Cem Concr Compos*, 45 (2014) 136–147. ISSN 0958-9465. https://doi.org/10.1016/j.cemconcomp.2013.09.003.

[7] Farid S A & Zaheer M M, Production of new generation and sustainable concrete using rice husk ash (RHA): A review. ISSN 2214-7853. https://doi.org/10.1016/j.matpr.2023.06.034.

[8] Meraz M M, Mim N J, Mehedi M T, Noroozinejad Farsangi E, Arafin S A K, Shrestha R K & Hussain M S, On the utilization of Rice husk ash in high-performance fiber reinforced concrete (hpfrc) to reduce silica fume content, *Constr Build Mater*, 369 (2023) 130576. ISSN 0950-0618. https://doi.org/10.1016/j.conbuildmat.2023.130576.

[9] Elfaleh I, Abbassi F, Habibi M, Ahmad F, Guedri M, Nasri M & Garnier C, A comprehensive review of natural fibers and their composites: An eco-friendly alternative to conventional materials, *Results in Engineering*, 19 (2023) 101271. ISSN 2590-1230. https://doi.org/10.1016/j.rineng.2023.101271.

[10] Martinelli F R B, Ribeiro F R C, Marvila M T, Monteiro S N, Filho F d C G & Azevedo A R G d, A review of the use of coconut fiber in cement composites, *Polymers*, 15(5) (2023) 1309. ISSN 2073-4360. https://doi.org/10.3390/polym15051309.

[11] de J Jiménez-García E et al., A low environmental impact admixture for the elaboration of unfired clay building bricks, *Constr Build Mater*, 407. https://doi.org/10.1016/j.conbuildmat.2023.133470.

[12] Pinheiro V D, Alexandre J, Xavier G d C, Marvila M T, Monteiro S N & de Azevedo A R G, Methods for evaluating pozzolanic reactivity in calcined clays: A review, *Materials*, 16(13) (2023) 4778. ISSN 1996-1944. https://doi.org/10.3390/ma16134778.

[13] Bamaga S O, A review on the utilization of date palm fibers as inclusion in concrete and mortar, *Fibers*, 10(4) (2022) 35. ISSN 2079-6439. https://doi.org/10.3390/fib10040035.

[14] Nayak J R, Bochen J & Gołaszewska M, Experimental studies on the effect of natural and synthetic fibers on properties of fresh and hardened mortar, *Constr Build Mater*, 347 (2022) 128550. ISSN 0950-0618. https://doi.org/10.1016/j.conbuildmat.2022.128550.

[15] Oyekan G L & Kamiyo O M, A study on the engineering properties of sandcrete blocks produced with rice husk ash blended cement, *Journal of Engineering and Technology Research*, 3(3). URL https://www.semanticscholar.org/paper/A-study-on-the-engineering-properties-of-sandcrete-Oyekan-Kamiyo/8956da1caa8c32762d3d8d4bc38cfb550b565c7a.

[16] Mishra L & Basu G. *Coconut fibre: Its structure, properties and applications*, vol. 1. Elsevier (2020). ISBN 9780128183984, pp. 231–255. https://doi.org/10.1016/b978-0-12-818398-4.00010-4.

[17] Hafidh S A, Abdullah T A, Hashim F G & Mohmoud B K, Effect of adding sawdust to cement on its thermal conductivity and compressive strength, *IOP Conf Ser Mater Sci Eng*, 1094(1) (2021) 012047. ISSN 1757-899X. https://doi.org/10.1088/1757-899x/1094/1/012047.

[18] Singh S, Dalbehera M M, Maiti S, Bisht R S, Balam N B & Panigrahi S K, Investigation of agro-forestry and construction demolition wastes in alkali-activated fly ash bricks as sustainable building materials, *Waste Management*, 159 (2023) 114–124. ISSN 0956-053X. https://doi.org/10.1016/j.wasman.2023.01.031.

[19] Rajapakse A M & Mudunkotuwa D Y, Cement and clay bricks reinforced with coconut fiber and fiber dust (2022) 233–248. ISSN 2773-7098. https://doi.org/10.31357/ait.v2i3.5534.

[20] Paul I, Oyewole O & Kizito M. Review of the utilization of waste biomaterial resources of selected food crops: Rice, Cassava, Cocoa, Sorghum and Oil Palm (2021). URL https://imt-mines-albi.hal.science/hal-03152418/, accessed: Nov. 12.

[21] Khan M A, Khan S A, Khan B, Shahzada K, Althoey F & Deifalla A F, Investigating the feasibility of producing sustainable and compatible binder using marble waste, fly ash, and rice husk ash: A comprehensive research for material characteristics and production, *Results in Engineering*, 20 (2023) 101435. ISSN 2590-1230. https://doi.org/10.1016/j.rineng.2023.101435.

[22] Rabehi B, Ghernouti Y & Boumchedda K, Strength and compressive behaviour of ultra high-performance fibre-reinforced concrete (UHPFRC) incorporating Algerian calcined clays as pozzolanic materials and silica fume, *European Journal of Environmental and Civil Engineering*, 17(8) (2013) 599–615. ISSN 2116-7214. https://doi.org/10.1080/19648189.2013.802998.

[23] Singh H, Brar G S & Mudahar G S, Evaluation of characteristics of fly ash-reinforced clay bricks as building material, *J Build Phys*, 40(6) (2017) 530–543. ISSN 1744-2583. https://doi.org/10.1177/1744259116659662.

[24] Codispoti R, Oliveira D V, Olivito R S, Lourenço P B & Fangueiro R, Mechanical performance of natural fiber-reinforced composites for the strengthening of masonry, *Compos B Eng*, 77 (2015) 74–83. ISSN 1359-8368. https://doi.org/10.1016/j.compositesb.2015.03.021.

[25] Ojo O J, Adepoju S A & Alhassan N, Geochemical and mineralogical studies of Kaolinitic clays in parts of Ilorin, Southwestern basement rock area, Nigeria, *Universal Journal of Geoscience*, 2(7) (2014) 212–221. ISSN 2331-9615. https://doi.org/10.13189/ujg.2014.020704.

[26] Oyelami C A & Rooy J L V, Mineralogical characterisation of tropical residual soils from south-western Nigeria and its impact on earth building bricks, *Environ Earth Sci*, 77(5). ISSN 1866-6299. https://doi.org/10.1007/s12665-018-7354-1.

[27] Mesele H, Grum B, Aregay G & Berhe G T, Evaluation and comparison of infiltration models for estimating infiltration capacity of different textures of irrigated soils, 13(1). ISSN 2193-2697. https://doi.org/10.1186/s40068-024-00356-5.

[28] Jasrotia P, Kbs058: Particle size analysis for soil texture determination (Hydrometer method). https://doi.org/10.1520/d0422-63r07.

[29] Astm C , Astm c 39/c 39m – 01. standard test method for compressive strength of cylindrical concrete specimens. https://doi.org/10.1520/c0039_c0039m-21.

[30] Mustapha K, Annan E, Azeko S T, Kana M G Z & Soboyejo W O, Strength and fracture toughness of earth-based natural fiber-reinforced composites, *J Compos Mater*, 50(9) (2016) 1145–1160. ISSN 1530-793X. https://doi.org/10.1177/0021998315589769.

[31] ASTM-E399, E399-17 standard test method for linear-elastic plane-strain fracture toughness, *Annual Book of ASTM Standards*, 90 (2017) 1–33. https://doi.org/10.1520/E0399-09E02.2.

[32] Li S, Yin J & Zhang G, Experimental investigation on optimization of vegetation performance of porous sea sand concrete mixtures by pH adjustment, *Constr Build Mater*, 249 (2020) 118775. ISSN 0950-0618. https://doi.org/10.1016/j.conbuildmat.2020.118775.

[33] Aneke F I, Awuzie B O, Mostafa M M H & Okorafor C, Durability assessment and microstructure of high-strength performance bricks produced from pet waste and foundry sand, *Materials*, 14(19) (2021) 5635. ISSN 1996-1944. https://doi.org/10.3390/ma14195635.

[34] Murmu A L & Patel A, Towards sustainable bricks production: An overview, 165 (2018) 112–125. ISSN 0950-0618. https://doi.org/10.1016/j.conbuildmat.2018.01.038.

[35] Wang S, Gainey L, Baxter D, Wang X, Mackinnon I D R & Xi Y, Thermal behaviours of clay mixtures during brick firing: A combined study of in-situ XRD, TGA and thermal dilatometry, *Constr Build Mater*, 299 (2021) 124319. ISSN 0950-0618. https://doi.org/10.1016/j.conbuildmat.2021.124319.

[36] Nadeau P H, Tait J M, McHardy W J & Wilson M J, Interstratified xrd characteristics of physical mixtures of elementary clay particles, *Clay Miner*, 19(1) (1984) 67–76. ISSN 1471-8030. https://doi.org/10.1180/claymin.1984.019.1.07.

[37] Siddika A, Mamun M A A, Alyousef R & Mohammadhosseini H, State-of-the-art-review on rice husk ash: A supplementary cementitious material in concrete, *Journal of King Saud University - Engineering Sciences*, 13(5) (2021) 294–307. ISSN 1018-3639. https://doi.org/10.1016/j.jksues.2020.10.006.

[38] Yiosese A O, Quality assessment of sandcrete blocks produced along-oke fomo area, Ilorin, Kwara state, *LAUTECH Journal of Civil and Environmental Studies*, 7(1). ISSN 2651-5628. https://doi.org/10.36108/laujoces/1202.70.0111.

[39] Rocha D L, Júnior L U D T, Marvila M T, Pereira E C, Souza D & de Azevedo A R G, A review of the use of natural fibers in cement composites: Concepts, applications and Brazilian history, *Polymers*, 4(10) (2022) 2043. ISSN 2073-4360. https://doi.org/10.3390/polym14102043.

[40] Donkor P, Obonyo E & Ferraro C, Fiber reinforced compressed earth blocks: Evaluating flexural strength characteristics using short flexural beams, *Materials*, 14(22) (2021) 6906. ISSN 1996-1944. https://doi.org/10.3390/ma14226906.

[41] Mustapha K, Azeko S T, Annan E, Kana M G Z, Daniel L & Soboyejo W O, Pull-out behavior of natural fiber from earth-based matrix, *J Compos Mater*, 50(25) (2016) 3539–3550. ISSN 1530-793X. https://doi.org/10.1177/0021998315622247.